Shape-Tailored Semiconductor Dot-in-rods: Optimizing CdS-Shell Growth for Enhanced Chiroptical Properties via the Rationalization of the Role of Temperature and Time

Junjie Hao,[a,b,e†] Peizhao Liu,[c,h†] Ziming Zhou,[c†] Haochen Liu,[c†] Wei Chen,[c,d,f] Peter Müller-Buschbaum,[f,g] Jiaji Cheng,[h] Kai Wang,[c] Xiao Wei Sun,[c*] Jean-Pierre Delville,[b*] Marie-Helene Delville[a*]

a. Univ. Bordeaux, CNRS, Bordeaux INP, ICMCB, UMR 5026, F-33600 Pessac, France.

b. Univ. Bordeaux, CNRS, LOMA, UMR 5798, 33405 Talence, France.

c. Institute of Nanoscience and Applications, Department of Electrical and Electronic Engineering, Southern University of Science and Technology, Shenzhen, 518055, China.

d. College of Engineering Physics, Shenzhen Technology University, Shenzhen, 518118, China.

e. College of Integrated Circuits and Optoelectronic Chips, Shenzhen Technology University, Shenzhen, 518118, China.

f. Technical University of Munich, TUM School of Natural Sciences, Department of Physics, Chair for Functional Materials, James-Franck-Str. 1, 85748 Garching, Germany.

g. Heinz Maier-Leibnitz Zentrum (MLZ), Technical University of Munich, Lichtenbergstraße 1, 85748 Garching, Germany;

h. Key Laboratory for the Green Preparation and Application of Functional Materials, Ministry of Education, School of Materials Science and Engineering, Hubei University, Wuhan, 430062, China.

*Address correspondence to marie-helene.delville@icmcb.cnrs.fr; jean-pierre.delville@u-bordeaux.fr; sunxw@sustech.edu.cn

FIGURES

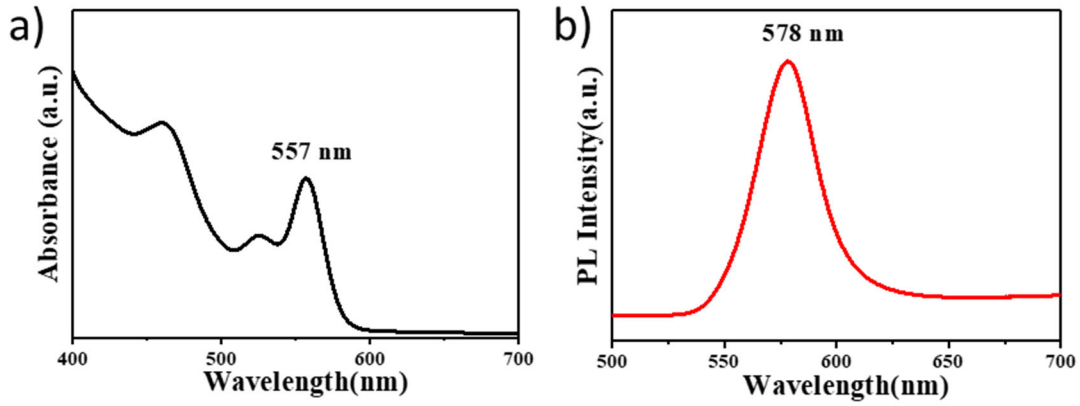

Figure S1. a) UV-vis absorption spectrum and b) PL emission spectrum of WZ-CdSe cores (λ_{abs} = 557 nm).

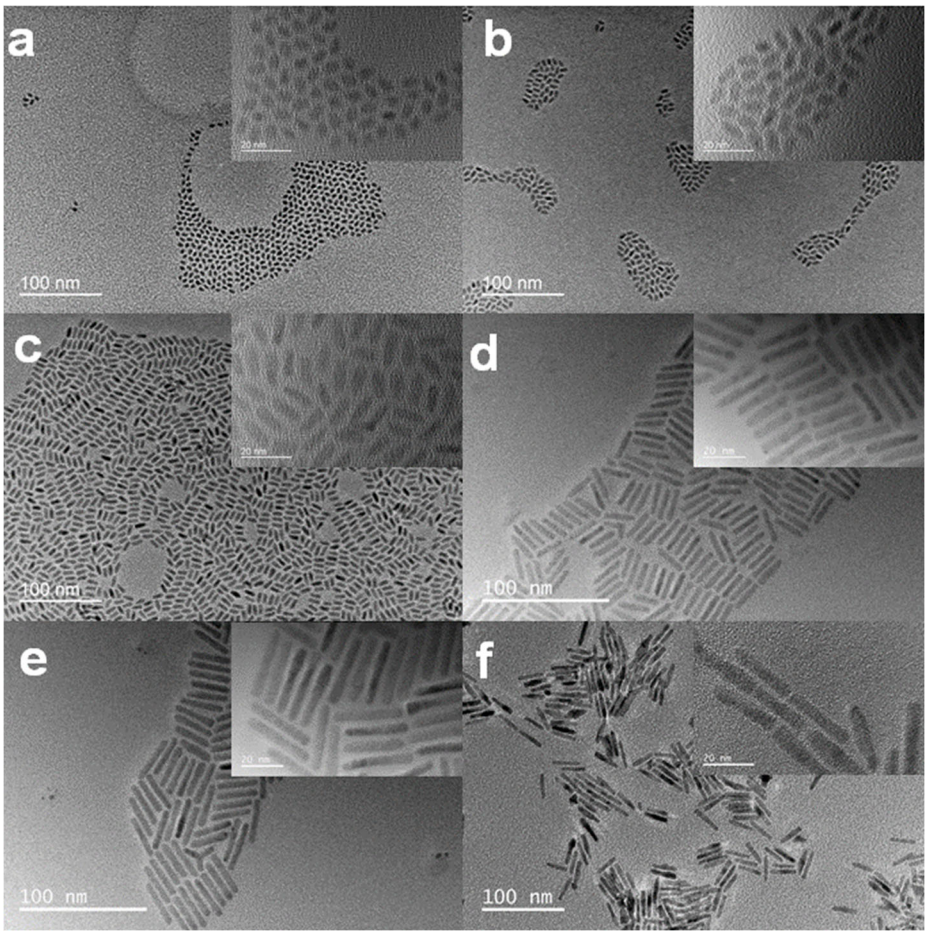

Figure S2. TEM images of DRs (7 to 12 in Table 3) synthesised at different temperatures using the same CdSe cores. a) 503 K, b) 533 K, c) 563 K, d) 593 K, e) 623 K, and f) 653 K.

Influence of initial thermal conditions on shell growth

Since, on the one hand, the temperature of the reactor plays a crucial role in the growth of CdS on the CdSe core, and on the other hand, the CdS shell thickness almost does not grow during the 1-d growth regime, control over this shell thickness is necessarily driven by the robustness of the experimental conditions from the beginning of the first isotropic growth stage onto the CdSe core, and such requirements are difficult to fulfill as growth is performed at high temperature. For instance, when injection of the shell precursors is performed into the reactor initially regulated in temperature at 593 K, the temperature transiently decreases to about 560 K and then returns to the setpoint temperature of the reactor after some transient recovery time of 40 s. The duration of this transient as well as the temperature difference to recover the thermal equilibrium likely determine the overall shell thickness before reaching the 1d-growth regime. This was assessed by control experiments, with two different heating mantle powers (see experimental section) and heating rates of 12 and ~5 K/min, respectively. T = 593 K was chosen as the reference reaction temperature and a concentration [CdSe] = 14 µM was selected to reach an aspect ratio AR close to 10. Under such conditions, recovery times of 40 s and 140 s, after the precursor injection, were required to come back to the setpoint temperature T = 593 K. CdSe/CdS DRs with 0.8 nm shells were formed at 90 W (5 K/min, DR-21) while 0.35 nm shells were obtained at 180 W (12 K/min, DR-5) (**Table S1**).

Table S1. Physical properties of CdSe/CdS DRs under different reaction times (based on the same CdSe core (D = 3.2 nm), with two heating power systems. Working temperature 593 K.

Name	[Core] µM	Power (W)	Reaction time (s)	Length (nm)	Diameter (nm)	Aspect ratio (AR)	Shell-thickness (nm)	Volume (nm^3)
DR-3		180	120	15.7±3.0	3.6±0.4	4.4	0.2	147.6
DR-4	14	180	240	21.0±2.7	3.8±0.4	5.5	0.3	223.8
DR-5		180	480	38.7±3.5	3.9±0.4	10.8	0.35	381.4
DR-19		90	120	14.9±3.7	4.3±0.6	3.5	0.55	195.6
DR-20	13	90	240	17.5±2.8	4.7±1.0	3.7	0.75	279.9
DR-21		90	480	26.2±2.2	4.8±0.5	5.5	0.80	445.2

* Overall volume $V = \pi D^2 (L - D/3)/4$, assuming a cylindrical shape with hemispherical ends.

We can thus infer that this increase in shell thickness is due to the prolonged delay, from 1 to 4 min. In short, the higher the heating system power, the shorter the transient recovery time and the thinner the shell of the DRs when switching to the 1d-growth regime. Similarly, the difference between the summer and winter temperature of the lab room was sufficient to provide CdSe/CdS DRs with shell thicknesses of 0.3 nm in summer and 0.6 nm in winter, simply because a decrease in the ambient temperature, increasing the temperature imbalance between the injected shell precursor and the reactor, and then the time required to recover the setpoint temperature of the reactor (**Table S2**). These two aspects may explain the variability of the results given in **Figure 1** and **Table 1**. Therefore to obtain CdSe/CdS DRs with significantly improved reproducibility, it is mandatory to work with a high-power heating mantle (180 W), to keep the temperature of the shell precursor solution constant, and to ideally make this temperature "as high as possible" to reduce both temperature imbalance and transient recovery time when thin shells are required.

Table S2. Physical properties of CdSe/CdS DRs under different ambient temperatures based on the same CdSe core (D = 3.2 nm). The core concentration was 18.8 µM, and the injection temperature was 593 K.

Name	Ambient temperature (K)	Length (nm)	Diameter (nm)	Aspect ratio (AR)	Shell-thickness (nm)	Volume (nm^3)
DR-10	303	24.3±1.6	3.8±0.4	6.4	0.3	261.2
DR-22	291	24.5±2.0	4.4±0.5	5.6	0.6	350.2

Using this method, it is also possible to extend the panel of colored DRs with a thin shell (green DR-16, orange DR-15, red DR-17, and DR-18) using different sizes of CdSe cores (**Table S3**, **Figures S3,** and **S4**). To keep the DRs with similar aspect ratios, the smallest cores required higher CdSe precursor concentrations.

Table S3. Characterizations of the thin shell CdSe/CdS DRs using different sizes of CdSe cores.

Name	CdSe core size (nm)	[CdSe core] µM	Length (nm)	Diameter (nm)	Aspect ratio (AR)	Shell-thickness (nm)	Volume (nm^3)
DR-16	2.2	91.2	14.0±3.1	2.9±0.4	4.8	0.35	86.1
DR-15	3.2	36.5	18.3±2.8	3.8±0.6	4.8	0.3	193.2
DR-17	3.9	12.4	23.9±2.5	4.2±0.4	5.7	0.15	311.7
DR-18	4.7	5.6	26.3±2.5	5.1±0.5	5.2	0.2	502.5

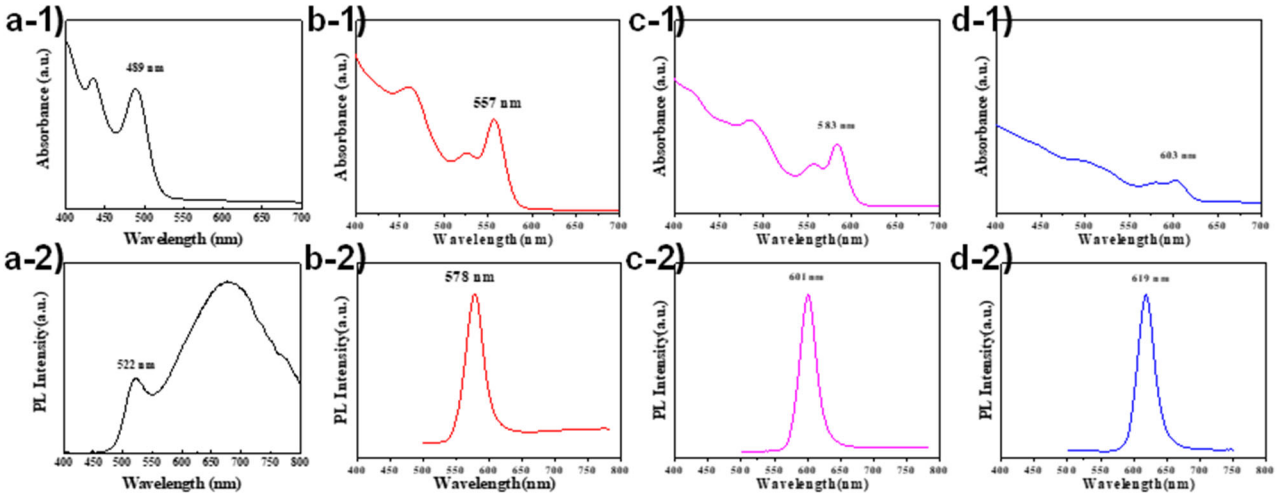

Figure S3. UV-vis absorption spectra and PL emission spectra of CdSe cores with different sizes. Abs = 489 nm (a), 557 nm (b), 583 nm (c), and 603 nm (d).

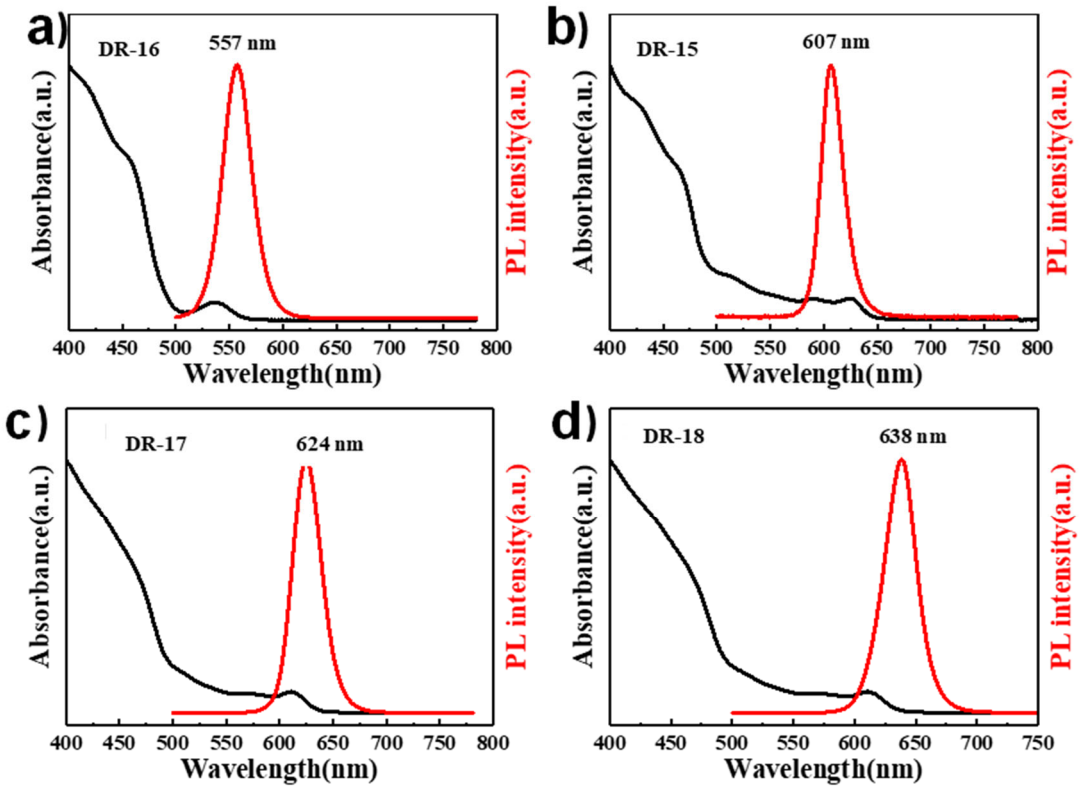

Figure S4. UV-vis absorption spectra and PL emission spectra of CdSe/CdS DRs with thin shell multi-color. a) DR-16 (green), b) DR-15 (orange), c) DR-17 (red), d) DR-18 (red).

Table S4. Physical properties of CdSe/CdS with different shell thicknesses based on the same CdSe cores (D = 3.2 nm).

Name	Length (nm)	Diameter (nm)	Aspect ratio (AR)	Shell-thickness (nm)
DR-10	24.3±1.6	3.8±0.4	6.4	0.3
DR-11	32.5±2.0	4.9±0.5	6.6	0.85
DR-12	30.4±2.5	5.8±0.8	5.2	1.3
DR-23	25.2±2.0	7.2±0.7	3.5	2.0

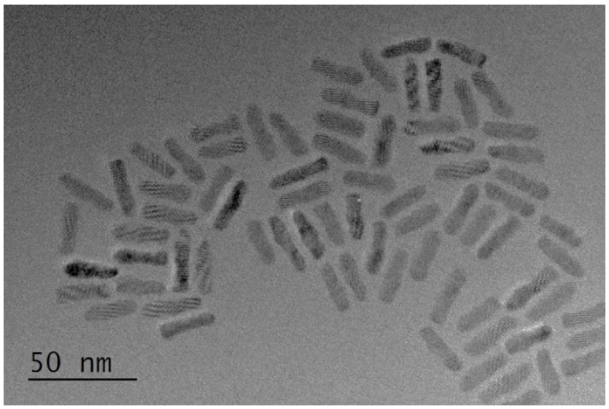

Figure S5. TEM image of DR-23 with a second over-coating process, the shell thickness is 2.0 nm.

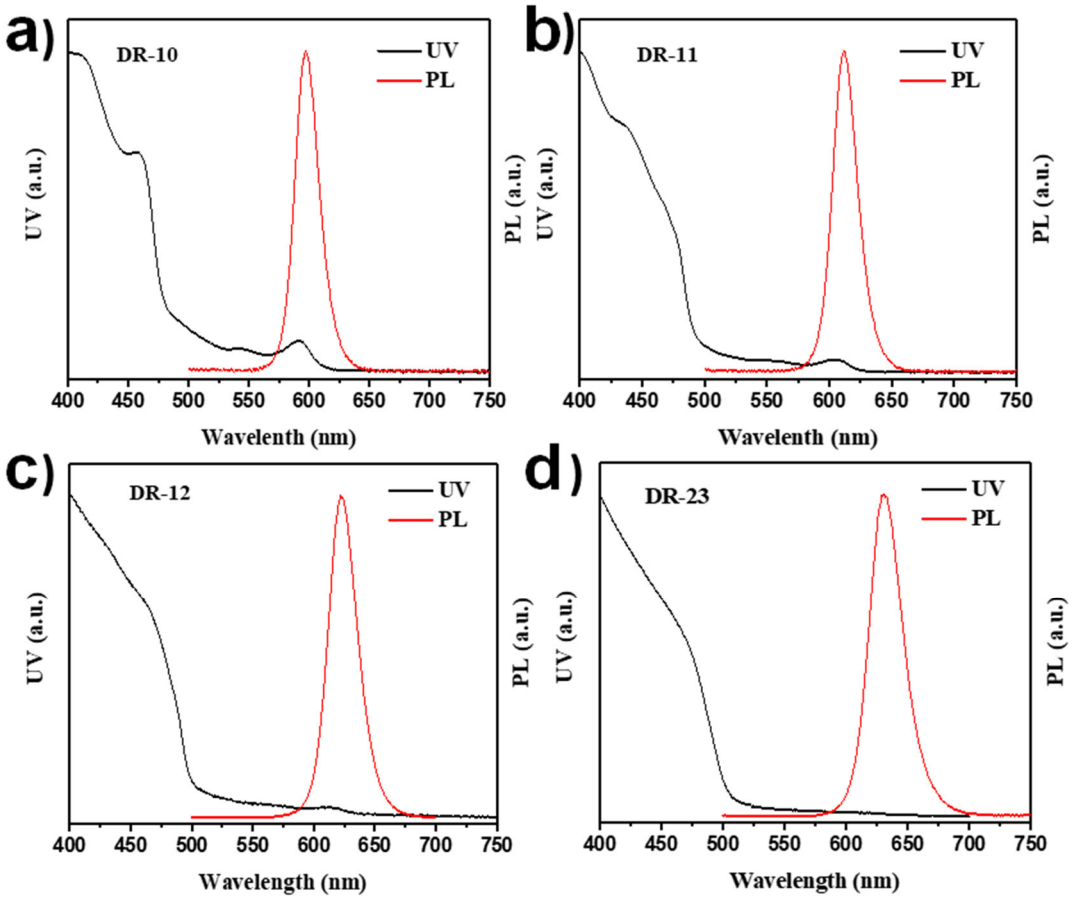

Figure S6. UV-vis absorption spectra and PL emission spectra of CdSe/CdS DRs with different shell thicknesses. a) DR-10, b) DR-11, c) DR-12, d) DR-23.

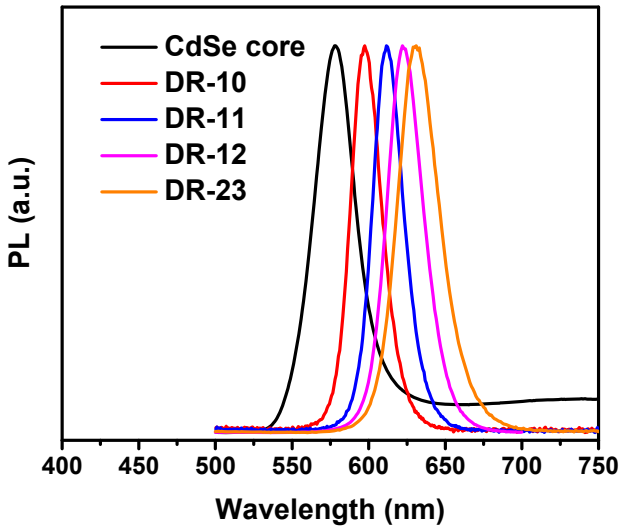

Figure S7. Variation of PL emission spectra of CdSe/CdS DRs with different shell thicknesses.

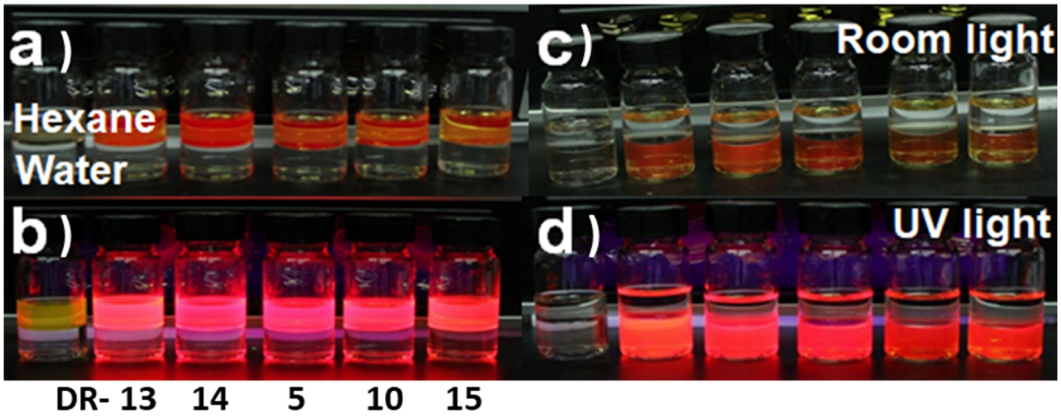

Figure S8. Images comparing the luminescence before and after the ligands exchange. (a, b) The oil phase QDs and DRs in hexane; (c, d) the aqueous phase QDs and DRs. Images (a) and (c), are under natural light, and (b) and (d) are under UV light (365 nm). From left to right: the CdSe QDs, and DRs with different aspect ratios (see Table 4 for details).

Table S5. The CD anisotropy factors of D-CdSe/CdS DRs with different shell thicknesses based on the same CdSe cores (D = 3.2 nm).

Name	g_{CD+}/λ_{CD}[a]	g_{CD-}/λ_{CD}[b]
DR-10	7.04×10^{-4}/473.4	-3.34×10^{-4}/454.6
DR-11	6.10×10^{-4}/485.2	-2.08×10^{-4}/468.8
DR-12	3.15×10^{-4}/484.8	-1.07×10^{-4}/464.6
DR-23	0.27×10^{-4}/488.0	-0.42×10^{-4}/474.9

[wa, b] CD anisotropy gCD-factors at the most intense positive and negative CD bands (nm).

Table S6. The CD anisotropy factors of L-CdSe/CdS DRs with different shell thicknesses based on the same CdSe cores (D = 3.2 nm).

Name	g_{CD+}/λ_{CD}[a]	g_{CD-}/λ_{CD}[b]
DR-10	4.52×10^{-4}/454.1	-8.79×10^{-4}/472.3
DR-11	1.76×10^{-4}/469.0	-6.24×10^{-4}/485.4
DR-12	1.37×10^{-4}/463.2	-3.42×10^{-4}/484.6
DR-23	0.15×10^{-4}/474.3	-1.34×10^{-4}/490.1

[a, b] CD anisotropy gCD-factors at the most intense positive and negative CD bands (nm).

Table S7. CD anisotropy factors of D-CdSe/CdS DRs under different core concentrations based on the same CdSe cores (D = 3.2 nm).

Name	g_{CD+}/λ_{CD}[a]	g_{CD-}/λ_{CD}[b]
DR-13	12.29×10^{-4}/478.8	-5.39×10^{-4}/459.8
DR-14	12.79×10^{-4}/475.9	-5.64×10^{-4}/456.7
DR-5	10.29×10^{-4}/474.0	-4.87×10^{-4}/455.4
DR-10	7.04×10^{-4}/473.4	-3.34×10^{-4}/454.6
DR-15	2.27×10^{-4}/475.8	-0.98×10^{-4}/453.4

a, b CD anisotropy gCD-factors at the most intense positive and negative CD bands (nm).

Table S8. CD anisotropy factors of L-CdSe/CdS DRs under different core concentrations based on the same CdSe cores (D = 3.2 nm).

Name	g_{CD+}/λ_{CD}[a]	g_{CD-}/λ_{CD}[b]
DR-13	5.48×10^{-4}/460.3	-12.13×10^{-4}/478.5
DR-14	5.85×10^{-4}/456.8	-12.96×10^{-4}/476.0
DR-5	5.00×10^{-4}/455.2	-10.24×10^{-4}/474.2
DR-10	4.52×10^{-4}/454.1	-8.79×10^{-4}/472.3
DR-15	0.95×10^{-4}/454.6	-2.39×10^{-4}/477.0

a, b CD anisotropy gCD-factors at the most intense positive and negative CD bands (nm).